Adsorption of asphaltenes on multiscale porous alumina

André Morgado Lopes, Véronique Wernert, Loïc Sorbier, Vincent Lecocq, Renaud Denoyel

Adsorption of asphaltenes on multiscale porous alumina

André Morgado Lopes[a,b], Véronique Wernert[a*], Loïc Sorbier[b], Vincent Lecocq[b], Renaud Denoyel[a]

[a]Aix-Marseille Université, CNRS, MADIREL, UMR 7246, Centre Saint-Jérôme, F-13397, Marseille cedex 20, France

[b]IFP Energies nouvelles, Rond-point de l'échangeur de Solaize, BP 3, 69360 Solaize, France

*Corresponding author: Dr. Véronique Wernert, veronique.wernert@univ-amu.fr

Abstract

Alumina catalysts are frequently used in refineries for the hydrotreatment of heavy petroleum fraction that are enriched in asphaltenes. The transport of real and model asphaltenes molecules through powder and alumina's extrudates treated or not at 150°C to remove or not surface-adsorbed water was studied. The kinetics and isotherms of adsorption at 298 K were obtained by the solution depletion method. Calorimetric experiments were also investigated. The kinetic is faster on the powder than on the alumina extrudates where the equilibrium is reached after 24 hours (against 1 hour for the powder) due to mass transfer limitation. The capacity of adsorption of model asphaltenes on untreated powder and extrudates is comparable around 1.1 and 1.2 $mg.m^{-2}$ and increases with the heat treatment due to water removal. Both adsorption strength and capacity of real asphaltenes on alumina is lower compared to the model asphaltene molecule which could be explained by the strong interaction between the acidic function of the model molecule and the alumina surface. The calorimetric study in absence of alumina shows the dimerization of model asphaltene molecules. In presence of alumina, the enthalpy of adsorption of model and real asphaltenes on alumina is determined. The enthalpy of adsorption of model asphaltenes on treated powder is higher than on untreated powder meaning that more energetic sites are available (probably due to the release of water-occupied sites) and the curve obtained for treated powder suggests different adsorption sites. The enthalpy of adsorption of model asphaltene is higher for the treated extrudates but these results must be taken carefully because the kinetic of adsorption is very slow (24 hours) for extrudates. The effect of flow rate was studied by saturating an extrudate column with model asphaltene molecules. The adsorption increases as the flow rate decreases which could be explained by higher friction in the macropores leading to the release of weakly retained asphaltenes as the flow rate increases or by less intermediate pore blocking by asphaltenes as the flow rate and thus the pressure increases. This study shows that the transport of asphaltenes through porous alumina supports is a complex process depending on many parameters.

Keywords: asphaltenes, alumina, adsorption, kinetics, isotherms, calorimetry, flow rate

1. Introduction

The behavior of asphaltene molecules in concentrated solutions has been a fertile topic for researchers in the oil and gas field for quite some time [1]. Knowledge of the general behavior of this molecular family is extensive but nevertheless incomplete. The complex nature of their characterization is the result of a series of interrelating features of the asphaltene family: these are heavy polyaromatic molecules often containing heteroatoms (nitrogen, oxygen, sulfur and metals) and have complex intermolecular interactions such as aggregation in bulk as well as adsorptive interactions with surfaces. The main differentiating feature of asphaltenes from other heavy hydrocarbons is their insolubility in normal paraffins [2]. Aggregation behavior has been a

major driver of research on asphaltenes, as it directly correlates with problems observed at the industrial scale such as clogging of catalysts, deposition and sedimentation within pipelines, among other undesirable effects [3,4]. Different techniques have been used to characterize multiple dimensions of the asphaltene problem. Small-angle scattering techniques have been essential in describing the clustering of asphaltene molecules, leading to the now well-established Yen-Mullins model [4,5]. According to this model, asphaltene aggregation follows a two-step process. In the first phase, up to 10 asphaltene molecules can stack parallel to each other, their polyaromatic cores forming π-π bonds due to the polarity of the delocalized electrons in the p-orbitals. These nanoaggregates can, at a second stage, clump together with other nanoaggregates, forming what are called "clusters". Asphaltene clusters can be significantly large – up to 200 times the molecular weight of an average single asphaltene molecule – however, clusters only tend to form at concentrations higher than 3000 ppm while nanoaggregates can form at concentrations as low as 50 to 200 ppm [6].

The aggregation behavior will often depend on the many possible combinations of different asphaltene molecules present in the solution as well as on the adsorptive properties of the surfaces around which these molecules percolate because adsorption can modify solution composition and provoke aggregation at the interface [7]. As such, studies which purport to describe asphaltene behavior, are most likely describing an observed average of the behavior of many different molecules. Aiming to narrow down the scope of analysis and mitigate complicating factors, articles have been published studying solutions comprised of a single asphaltene molecular structure [8-10] supposed to be representative of actual ones. These studies focused on the interactions of synthesized asphaltene analogues with different surfaces representative of substrates encountered at different stages in the lifecycle of asphaltene molecules. This article complements these efforts by adding alumina as a surface of interest. The importance of studying the interactions between asphaltenes and alumina cannot be understated, as this material is frequently used as a catalyst support in the hydrotreatment of heavy petroleum fractions in refineries [11]. A more thorough comprehension of the transport of molecules of this family could lead to the optimization of these processes via the fine tuning of the catalyst support characteristics, potentially resulting in significant yield gains.

2. Experimental section

2.1. Alumina surfaces

Experiments were performed with both a mesoporous alumina powder and multiscale porous alumina extrudates. The powder sample was aluminum oxide Me90 standardized for chromatographic adsorption analysis with a neutral pH provided by Merck. The particles have a spherical shape and radii between 63 and 200 μm. The γ-alumina porous extrudates, manufactured by IFPEN (Solaize, France) using the sol-gel method, were used, and fully characterized in a previous study [12]. The extrudates have a cylindrical shape with a radius of

0.94 mm and an average length of 15 mm and will be called 360Mono. Unlike the extrudates used in industrial applications these extrudates were not impregnated with active sites, in order to isolate diffusion and adsorption effects and prevent the formation of foreign species. The topological characteristics of both solids are present in Table 1.

2.2. Asphaltenes

A model asphaltene molecule has been used to simulate the behavior of asphaltenes through the alumina supports. This model molecule (henceforth referred to as C5PeC11) has been synthesized at the Ugelstad Laboratory, Norwegian University of Science and Technology. This molecule is a continental-type asphaltene [13] with a central aromatic island identical to that of pigment Violet 29. Additionally, it has aliphatic groups on either side of the central polyaromatic structure, one of them ending in a carboxyl acid functional group. This adds up to a molecular weight of 829.13 $g.mol^{-1}$. Previous experiments performed on this molecule [8-10] will be referenced throughout the results and discussion section. A representation of the model molecule is given in figure 9 when the dimerization is presented (see results part 3.2).

The results obtained with C5PeC11 were compared to a mixture of asphaltenes extracted from Safaniya (Saudi Arabia) crude with n-heptane (henceforth referred to as RC7), following the procedure specified on norm NF T60-115 [13].

2.3. Taylor dispersion analysis (TDA)

Taylor dispersion analysis is used to determine the molecular diffusion (D_m) of asphaltenes in toluene by studying the widening of the peak due to radial diffusion [14]. 10 µL of a C5PeC11 solution at 0.08 $g.L^{-1}$ in toluene were injected into short (5 cm) and long (150 cm) polytetrafluoroethylene capillaries with an internal diameter of 0.7 mm at flow rates of 0.5, 0.1 and 0.01 $ml.min^{-1}$. To ensure valid results, TDA experiments must be performed in proper conditions: a residence time, *t'*, in excess of what is necessary to let molecules diffuse radially from the center of the capillary to its edges; and a negligible contribution of the axial dispersion on the mass transfer (measured using the Péclet number - *Pe*). These conditions are specified in Equations 1 and 2, t_i is the shortest residence time of the system, r_c is the radius of the capillary and u is the linear velocity of the fluid.

$$\frac{t'}{t_i} = \frac{D_m t_i}{r_c^2} > 1.4 \qquad 1$$

$$Pe = \frac{u r_c}{D_m} > 70 \qquad 2$$

Equation 3 is used to calculate D_m, based on the differences in retention times (noted t) and variances (σ) of peaks with a short capillary (subscript i) and long capillary (subscript r).

$$D_m = \frac{r_c^2(t_r - t_i)}{24(\sigma_r^2 - \sigma_i^2)} \quad (3)$$

2.4. Adsorption isotherm and kinetics depletion method experiments

Both isotherms and kinetics of adsorption tests were carried out on the asphaltene model molecule C5PeC11 as well as RC7 asphaltene sample using the solution depletion method. Tests were done on both untreated alumina (which had been exposed to the uncontrolled atmospheric moisture) and treated alumina (from which this moisture was partially removed). To treat the alumina, it was set under a helium flow and heated to 150 °C using a sand bath. Asphaltenes were solubilized in toluene (purchased from Carlo Erba Reagents, Peypin, France) and injected into the vials containing the alumina solids.

All isotherms and kinetics experiments were performed at 25 °C. The vial with the solution and support is kept in a rotating mixer. After the exposure, solution samples were taken from the vials and their concentrations were measured via UV-Visible spectroscopy. Equation 4 was used to calculate the amount adsorbed per unit area, Γ_{ads}, in which m_s is the mass of solid, n_i and n_f are the initial and final amount of solute in the liquid phase, C_i and C_f are the initial and final concentrations, V_i and V_f are the initial and final volumes and a_s is the specific surface area determined by nitrogen adsorption à 77K.

$$\Gamma_{ads} = \frac{n_i - n_f}{a_s m_s} = \frac{C_i V_i - C_f V_f}{a_s m_s} \quad (4)$$

The mass of solid used for both powder and extrudates was 10 mg, placed in a volume of 1 mL of solution. In the experiments performed with heat treatment, the septa of the vials used was pierced twice to allow the helium to flow. This causes a small volume of toluene to evaporate over the course of the experiment. As such, the mass of the vial and its contents was measured before and after exposure to ascertain the amount of toluene evaporated.

2.5. Microcalorimetry

Microcalorimetry experiments were performed using a TA Instruments TAM III Tian-Calvet type microcalorimeter. Some extrudates was cut in small pieces for calorimetric experiments. The experimental apparatus comprises a reference and a sample cell on opposite sides of a heat sink, which keeps the system at isothermal conditions at a temperature of 25 °C. Stock solution is incrementally injected from a micrometric syringe in increments of 2 µL into a sample cell. The solution was well mixed, thanks to a gold propeller present in the sample cell. The heat flow for each injection step was measured by thermopiles surrounding both the sample and reference cells.

The experiments are divided into three steps: an initial blank experiment is performed where both the sample and reference cell contain only the solvent (toluene). Solvent is then injected into the

sample cell and the heat measured during this experiment corresponds to the heat caused by injection-related perturbations. These include the potential energy of the solvent falling into the cell, viscous effects, the compression of the vapor phase (given the addition of liquid into an otherwise closed system) which causes some condensation and any possible temperature gradients between the solvent in the syringe and the solvent in the cell, all of which are observed as a release of heat. This heat of injection is exothermal and must be subtracted from the experiments performed with asphaltene stock solution, both dilution and adsorption.

A dilution experiment where asphaltene stock solution is introduced to the sample cell with no adsorbent must be performed as well. The heat measured is equivalent to the enthalpy of dilution at each step, Δh_{dil}, of the asphaltenes from the stock solution concentration into pure toluene during the injections, as well as the heat of self-association of asphaltenes, which, again, are parallel effects to adsorption. Thus, in the adsorption experiment, where adsorbent is present inside the sample cell, the heat measured at each step of the titration is a convolution of the heat consumed by the dissociation and dilution as well as the heat released by the process of adsorption onto the surface. As such, the dilution enthalpy must be subtracted from the experimental heat measured at each injection in the adsorption experiments, Q_{exp}, which are performed with powder in the sample cell, to isolate the enthalpy of adsorption, Δh_{ads} (Equation5).

$$\mathrm{Q_{exp}} = \Delta \mathrm{h_{ads}} + \Delta \mathrm{h_{dil}} \qquad 5$$

The adsorption experiments were performed in the high affinity range of the adsorption isotherm – the initial concentration and amount of sample have been calculated such that equilibrium points fall in the high affinity region of the isotherm. The initial concentration of the stock solution was 2 $g.L^{-1}$ and the amount of solid in the cell during the adsorption experiments was 10 mg. The calculations were performed via the method described by Denoyel *et al.* (1990) [16].

$$\Delta \mathrm{H_{ads}} = \frac{\sum \Delta \mathrm{h_{ads}}}{\mathrm{n_i^a}} \qquad 6$$

Equation 6 allows us to calculate the enthalpy of adsorption, ΔH_{ads}, in which n_i^a is the adsorbed molar quantity present in the cell after step i. As the solution is injected into the sample cell, it is assumed that the process of dilution occurs to completion and is only then followed by the process of adsorption from batch. This simplifies the calculation of what quantity is adsorbed based on the isotherm of adsorption. To this end an equation, without any physical relevance, is used to fit the experimental data, given by Equation 7.

$$\Gamma_{\mathrm{ads}} = \mathrm{x_0} + \frac{\mathrm{x_1}}{1 + (\mathrm{C}/\mathrm{x_2})^{\mathrm{x_3}}} + \mathrm{x_4 e^{-C/x_5}} \qquad 7$$

Parameters x_0 through x_5 are chosen such that this model fits the experimental data. The amount adsorbed and the equilibrium concentration in the cell are deduced from this equation and the mass balance. From here, at each injection, the amount injected is calculated. The heat from

dilution already subtracted, what remains is the heat of adsorption which can be transformed in adsorption enthalpy per mole of substance.

2.6. Adsorption vs. flow rate tests

The apparent influence of flow rate on the adsorption was tested on a column made of extrudates previously saturated with C5PeC11 asphaltenes. The flow rates are set at 0.2 $ml.min^{-1}$ or 0.1 $ml.min^{-1}$ and the flow rate change are indicated in the legends of the figures 11 and 12. Columns manufactured with the alumina extrudates were used in the flow rate experiments. The column construction method was detailed in a previous paper [12]. These columns are connected to a Gilson 302-303 HPLC pump to facilitate the flow of asphaltene molecules through the extrudates.

Saturation is performed by recirculating a solution of 3 $g.L^{-1}$ of C5PeC11 in toluene through two columns, both built with a single extrudate for 72 hours (average column length of 1.48 ± 0.05 cm; average mass of alumina in each column is 31.10 ± 0.08 mg). The concentration was chosen to be in excess of the minimum equilibrium concentration required to achieve the plateau of the adsorption isotherm and the recirculation time was chosen, likewise, in accordance with kinetics of adsorption. Both are further explored in the results and discussion section.

The flow rate experiments force the flow of asphaltenes from a sealed container through column to an Agilent Cary 60 UV-Vis spectrophotometer detector set to continuously detect at a wavelength of 526 nm (the maximum spectral absorption peak for C5PeC11) using the Cary WinUV Kinetics software module. After detection, the outgoing solution loops back to the original vial to be recirculated. The concentration of the solution is chosen such that the UV-detector is not saturated (in the case of C5PeC11, below 0.4 $g.L^{-1}$) and the system was re-equilibrated at this concentration. The cell used was a flow-through cell with an optical path length of 10 mm. Figure 1 presents a simplified schematic of the setup.

3. Results and Discussion

3.1. Batch asphaltene adsorption experiments

Adsorption experiments were performed on both solids (powder and extrudates) with and without heat treatment (150 °C under helium). As the isotherms in Figure 2 show, C5PeC11 has a high affinity for the alumina surface, regardless of morphology or treatment.

Equation 8 shows the Langmuir model in its dimensionless form, with the concentration (C) compared to a reference state with concentration, C_0 = 1 $mol.L^{-1}$.

$$\Gamma_{ads} = \frac{\Gamma_{max} b_0 \frac{C}{C_0}}{1 + b_0 \frac{C}{C_0}} \quad (8)$$

Adjusting the maximum capacity, Γ_{max}, and affinity, b_0, parameters, the Langmuir model fits all the curves adequately and has been used on both the modelling of the adsorption of real asphaltene fractions [17,18] as well as the model asphaltenes used in this study [9]. Thermodynamically, b_0 is equivalent to the equilibrium constant of the adsorption mechanism, which means it can be used to calculate the Gibbs free energy, ΔG^0, via Equation 9 (T is temperature and R is the molar gas constant).

$$\Delta G^0 = -RT \ln b_0 \quad (9)$$

Table 2 shows the parameters which best fit the Langmuir model to the experimental results. Untreated extrudate and powder supports have a similar capacity, around 1.1 - 1.2 mg.m^{-2} while heat treated extrudates, unsurprisingly present a much higher capacity, as the water molecules which typically compete for adsorption sites with the asphaltene molecules [19,20] on the hydrophilic alumina surface are released when the sample is treated under the inert atmosphere and at high temperature. This leaves more of the alumina surface exposed as well as creating more energetic adsorption sites (as will be discussed later). For the purposes of these experiments, the treatment is performed at 150 °C, however thermogravimetric analysis shows that water is continuously released even at much higher temperatures, with only a slight inflexion point present close to the treatment temperature of 150 °C. It is, therefore, difficult to remove all the water adsorbed on alumina surfaces. Temperatures higher than 700 °C border on the phase change temperatures from γ-alumina into other crystalline phases.

Figure 3 shows a comparison between the adsorption behavior observed in alumina and different materials studied by Pradilla et al. [8]. Alumina and silica surfaces have similar surface capacities which is to be expected since they have the same functional interaction even if silica is weakly acidic and alumina is amphoteric (both acid and basic sites). Stainless steel and calcite have different surface chemistry and different interactions with the asphaltene molecules.

The kinetics of adsorption were determined using a solution of C5PeC11. Adsorption on the powder sample was predictably quick, as equilibrium was reached after around 60 minutes. For the extrudates, however, achieving equilibrium took much longer, at over 24 hours. The surface chemistry of the powder and extrudates is the same, therefore, it is safe to assume that these results are, in fact, not strictly related to the kinetics of adsorption, but indeed a combination of adsorption kinetics and the diffusion of the asphaltene molecules within the extrudate support, as they scour the surface for higher energy adsorption sites. Interestingly, the global kinetics were not affected by heat treatment, which again, supports the hypothesis that mass transfer limitations are the limiting factor, rather than the kinetics of adsorption, as seen in Figure 4.

Assuming an effective diffusion coefficient D_{eff} around 1×10^{-11} $m^2.s^{-1}$ (a value commonly seen in the literature [21]) one can calculate the characteristic time for diffusion, $t_d = d^2/D_{eff}$, with d being the characteristic length of each support. For the alumina porous particles, d is the particle diameter and for the extrudate d is the diameter of the whole extrudate. To estimate the value of t_d, D_{eff} has to be estimated in the mesoporous domain for the porous particles and in the mesoporous and macroporous domains for the extrudate. It is possible to verify that given the ratio of the particle to extrudate radius, it is expected that the kinetics observed with the extrudate sample should be at least 200 times slower than the powder sample. The D_{eff} values could be estimated in non-adsorbing conditions from the properties of the porous materials like the porosity (ε) and the tortuosity (τ). For the alumina porous particles, the asphaltene molecule have to diffuse through the alumina particles which have a diameter ranging between 63 and 200 µm and for the extrudate the asphaltene molecules have to diffuse through the whole extrudate meaning in the macroporous and mesoporous domains. For the extrudate support the D_{eff} values could be estimated in non-adsorbing conditions from the total porosity (ε_t), the total tortuosity (τ_t) and the molecular diffusion of the asphaltene molecule (D_m) according to $D_{eff}=\varepsilon_t.D_m/\tau_t$ with ε_t being 0.77 and total tortuosity being 2.4 [12]. The D_m value is obtained experimentally by TDA and is $4.7.10^{-10}$ $m^2.s^{-1}$ for the C5PeC11 model asphaltene molecules. For the C5PeC11 model asphaltene molecules, the calculated effective diffusion is then $1.3.10^{-10}$ $m^2.s^{-1}$ for the extrudate support. For the alumina particles the D_{eff} is the intraparticle diffusion coefficient which could be calculated in non-adsorbing conditions according to $D_{eff}=\varepsilon_p.k_f.D_m/\tau_p$ where ε_p is the intraparticle porosity (ε_p is 0.47 for the porous particles used), k_f is the friction coefficient which could be estimated with the Renkin equation ($k_f=1-2.104.(r_m/r_p)^3-0.95.(r_m/r_p)^5$) and τ_p is the particle tortuosity (τ_p is around 2 for alumina porous particles) [22]. The size of the model asphaltene molecules is 0.94 nm and the pore size is 5.1 nm. The D_{eff} value is about $1.4.10^{-11}$ $m^2.s^{-1}$. The D_{eff} value is higher for the extrudate support due to fast diffusion in the macroporous volume. The characteristic time is 456 min for the extrudate support and 47 min for the largest alumina porous particles (200 µm) and 5 min for the smallest particles (63 µm). The characteristic time t_d of the extrudate support is thus 10 to 100 times slower than with the porous alumina particles knowing that those estimations were made in non-adsorbing conditions.

As a point of comparison to the C5PeC11 model asphaltenes, a mixture of asphaltenes extracted from crude (dubbed RC7) was studied using the same methods. In terms of color, the dried RC7 is much closer to black and brown than the bright orange C5PeC11. In solution with toluene, this translates to a translucent sandy color at low concentration, evolving into darker and darker shades of caramel as concentration increases. At concentrations above 1 $g.L^{-1}$, the solution becomes opaque (Figure 5).

Experiments were performed with both untreated and heat-treated 360Mono extrudates as adsorbent with the same setup as the one used for the C5PeC11 experiments. Figure 6 displays

the results obtained as well as Langmuir model fits (parameters in Table 3) for both untreated and treated samples.

It is immediately evident that adsorption of RC7 in alumina is much weaker than the model molecule both in terms of affinity and capacity. The acidic functionalization in C5PeC11 interacts much more strongly with the alumina surface. Very low adsorption capacity for asphaltene mixtures is not uncommon in the literature [23]. It is strange, however, that treated alumina samples have a lower maximum capacity than the untreated alumina. In both cases, the plateau of adsorption was never experimentally observed. Gaulier et al [18] performed similar experiments with asphaltenes extracted from the same source by the same process and required concentrations at equilibrium of well above 4 $g.L^{-1}$ to achieve the isotherm plateau. It can be, therefore, assumed that at these relatively low concentrations, experimental errors are too great for accurate results. This does not mean that these results are without worth. The capacity and affinity of RC7 can definitively be said to be significantly lower than that observed with the C5PeC11 molecule, meaning that it alone cannot completely model the behavior of real asphaltene systems.

Kinetics of adsorption were also studied (Figure 7). Both untreated and treated samples seem to follow the same kinetics, with the same behavior displayed by C5PeC11. Consistent with what was previously shown, equilibrium with RC7 is also reached after roughly 24 hours. It is known that diffusional phenomena are the limiting factor in the kinetics, as such, these results somewhat imply that, on average, the diffusional properties of the C5PeC11 model molecule are similar to the ones of the extracted asphaltenes.

3.2. Microcalorimetry

Microcalorimetric studies were performed on the alumina powder as well as small pieces of extrudate with the procedure detailed in section 2.5. During the dilution measurement, it is observed that the heat released as the concentration of C5PeC11 increases in the sample cell follows a pattern expected from self-association, more specifically, dimerization. As the molecules in the high concentration stock solution enter the sample cell, they come in contact with the solvent at low concentrations and the molecules that would be dimerized in the stock solution dissociate, which is the source of the endothermal peaks observed.

$$(\mathrm{C5PeC11})_2 \leftrightarrow 2(\mathrm{C5PeC11}) \qquad 10$$

$$\mathrm{K_d} = \frac{[(\mathrm{C5PeC11})]^2}{[(\mathrm{C5PeC11})_2]} \qquad 11$$

Using the van t'Hoff equation (Equation12) it is possible to calculate the equilibrium constant of the dissociation reaction, K_d, from its relationship with the molar enthalpy of dissociation, ΔH_d.

$$\frac{d}{dT}\ln K_d = \frac{\Delta H_d}{RT^2} \quad (12)$$

In each step n of the calorimetric experiment, the total concentration of asphaltene molecules in the cell, $C_{cell,n}$, either monomers or dimers, is known and can be calculated using Equation 13, where C_S is the concentration of the stock solution, V_{inj} is the volume introduced per injection and V_i is the initial volume of solvent within the cell.

$$C_{cell,n} = [(C5PeC11)] + 2[(C5PeC11)_2] = \frac{C_S * nV_{inj}}{V_i + nV_{inj}} \quad (13)$$

Combining Equations 11, 12 and 13, as well as performing the mass balance described in Hallén et al. (1988) [24], gives us the enthalpy observed in each step, ΔH, given by Equation 14 :

$$\Delta H = \frac{\Delta H_d[(C5PeC11)]^2}{K_d C_{cell,n}} \quad (14)$$

The concentration of monomer in the cell is a function of the total concentration as well as K_d.

$$[C5PeC11] = \frac{\sqrt{K_d^2 + 8K_d C_{cell,n}} - K_d}{4} \quad (15)$$

Finally combining Equations 14 and 15 and algebraically simplifying, one finally obtains Equation 16:

$$\Delta H = \frac{\Delta H_d\left[K_d + 4(C_{cell,n} - C_S) - \sqrt{K_d^2 + 8K_d(C_{cell,n} - C_S)}\right]}{8(C_{cell,n} - C_S)} \quad (16)$$

This model fits well with the measurements suggesting that the hypothesis of dimer formation is correct. Figure 8 presents the experimental results as well as the model fit and Table 4 shows the parameters obtained, including the free energy of dissociation, ΔG_d, and the entropy, ΔS_d, calculated from Equation 17.

$$\Delta G_d = \Delta H_d - T\Delta S_d \quad (17)$$

The dissociation equilibrium constant is quite low, meaning the dimerization reaction is favored. At 2 g.L^{-1}, the initial concentration, around 50% of the asphaltenes molecules are present as dimers. Simon et al. (2016) [10] performed these same dilution experiments with stock solutions of C5PeC11 in xylene at different concentrations. The values were found to be in the same order of magnitude for both ΔH_d and ΔS_d, though, about twice as high as the values obtained in this study. This difference may be due to different solvent used (a xylene mixture).

The structure proposed by Simon et al. is a stacking of two asphaltene molecules with stacked aromatic rings (π-π bonds) as well as hydrogen bonds in the acidic functionalization (Figure 9).

This is confirmed in the paper by comparison with the heats of adsorption obtained for the dimerization of stearic acid (aliphatic compound with 18-carbon chain and one carboxylic acid functionalization).

Following the dilution study, the asphaltene solution was titrated with Me90 alumina powder and 360Mono extrudates in the sample cell. Results can be found in Figure 10.

There is a marked difference between the adsorption on untreated and treated powder. The alumina powder was treated to remove water and verify the low values of enthalpy of adsorption measured by calorimetry on the untreated powder. Similar isotherms of adsorption being obtained for untreated and treated powder in the high affinity range. The adsorption enthalpy at low concentrations is much higher for the treated powder, meaning a lot more energy is being released by the initial adsorption of asphaltenes. An enthalpy curve with the shape observed in the adsorption in treated powder is characteristic of heterogeneous systems, meaning there are different adsorption sites. The enthalpy measured is, in fact, an enthalpy of displacement encompassing the desorption of the solvent from the surface and the adsorption of the species in question, in this case C5PeC11 [15].

As previously discussed, heat treatment removes some of the water adsorbed in the alumina surface. As before, treatment consists in exposing the sample to a vacuum at 150 ºC, which, according to thermogravimetric results, removes about 50% of the water adsorbed in the alumina's hydrophilic surface. The desorption of water must, therefore account for some of the loss of energy released by the adsorption of asphaltenes in the untreated sample. These higher energy sites are filled by the first molecules arriving in the sample cell and, as concentration increases, newly arriving C5PeC11 must compete with the water still present after heat treatment for the remaining sites.

The trend is precisely the same in the extrudate sample, though there is a slight dip in the adsorption enthalpy at the start. The equilibration time used might not have been enough in the experiment with extrudates, especially given the highly diffusion-dependent kinetics of adsorption. However, the extrudates used in the calorimetry experiments was much smaller (length-wise and mass-wise) than the extrudates used in the batch adsorption isotherm experiments. Finally, the enthalpy of adsorption in the extrudates seems to be so much higher than the one obtained with the powder sample indicating a different surface chemistry between samples.

3.3 Flow rate tests

The apparent influence of the flow rate on adsorption was studied using the setup described in section 2.6. As with the HPLC measurements, concentrations at the plateau of the isotherm of adsorption were shown to saturate the UV-Vis detector. As such, the recirculating concentration was progressively lowered until the detector was no longer at risk of saturation. A blank was performed by connecting the pump directly to the cell. The initial flow rate was 0.2 $mL.min^{-1}$, the

same flow rate to be used with the columns made of extrudates. Due to the volume of the UV flow-through cell (0.113 mL), it is expected that the equilibrium time should be around 30 s. The blank experiment (without column) revealed that there is no influence of the flow rate on the measurement. A slight increase of absorbance is observed over time, caused by the slow evaporation of the toluene in the C5PeC11 solution which was corrected for in the experiments with column. Otherwise, the system is highly stable, as is shown in Figure 11, where A/A_0 is the absorbance, relative to the initial absorbance at t = 0.

With columns in the system, equilibrium time becomes even longer, as it must now account for the kinetics of adsorption. Experiments were performed on two previously saturated single-extrudate columns. Figure 12 shows the evolution of the absorbance over time in one of the experiments performed. Prior to the experiment, the absorbance is stable. The time t=0 corresponds to the time where the UV-visible signal was stable, and the column well equilibrated at a flow rate of 0.2 ml.min^{-1}. When the flow rate is changed from 0.2 to 0.1 mL.min^{-1}, the absorbance begins to slowly decrease. This implies a decrease in the concentration at the outlet of the column, thus, an increase in the amount of C5PeC11 adsorbed in the column. It's likely that the kinetics of adsorption in continuous flow conditions are different than what is observed in batch conditions. For the extrudates in batch conditions, diffusion is the limiting step when it comes to kinetics of adsorption. By comparison to the powder samples, the kinetics of adsorption on extrudate is several orders of magnitude slower. With the addition of flow, advective processes accelerate the dispersion of the solute through the extrudate. Even with this added mobility, kinetics are quite slow due to the high tortuosity of the extrudate porous network as measured in a previous study ($\tau_{LONGITUDINAL}$ = 2.39; $\tau_{TRANSVERSE}$ = 3.00) [12]. This means that even after 150 minutes, the new equilibrium state might not have been achieved. As the flow rate is set back to its original value, concentration increases, dramatically at first, suggesting a quick release of weakly adsorbed molecules. Molecules continue being desorbed over time until the concentration measured eventually returns to its initial value after 500 min.

Descriptions of adsorption behavior outside the time domain (i.e. adsorption kinetics) in the literature sit squarely and overwhelmingly within the domain of thermodynamics. As such, flow rate would, theoretically, have no influence on adsorption behavior whatsoever. Using front chromatography methods [26], Gritti and Guiochon observed a very small increase of amount adsorbed with higher flow rates. This effect was attributed to the increase in pressure within the column causing the equilibrium to become more favorable toward adsorption. This behavior is, in fact, the reverse of what is observed by the experiments above described.

The literature remains regrettably scarce on this subject. Other studies [27-29] have noted increases in amount adsorbed at equilibrium with lower flow rates but since these are breakthrough experiments, it is not certain that the final uptakes calculated for each flow rate are at equilibrium. Residence time is, therefore, the primary culprit for less adsorption at high flow rates. Aside from residence times, causes for adsorption fluctuations with flow rate are seldom discussed.

When it comes to the asphaltene situation, two related and possibly concurrent hypotheses are proposed. Higher flow rates increase friction on the surface of asphaltenes adsorbed in the macropores (where advection is the main form of mass transfer) which could release some of weakly adsorbed asphaltenes. These molecules may be only adsorbed on top of other asphaltenes through relatively weak π- π interactions, forming the stacked microaggregates discussed in the Yen-Mullins model. The first hypothesis posits that the shear force at higher flow rates is somehow enough to disaggregate and displace some of these asphaltenes which are weakly retained at lower flow rates.

Simultaneously, low flow rates may allow for deposition of asphaltenes aggregates in such a way as to block intermediate sized pores. This second hypothesis suggests that a sudden increase in the flow rate may apply enough pressure to break through these blockages, releasing the asphaltenes causing them. This would explain the sudden sharp increase in concentration observed at the outlet after the flow rate increase shown in Figure 12.

The drops in concentration are low enough that such hypotheses may be at least part of the cause of the observed phenomena. Figure 13 shows the concentrations obtained at the end of each experiment with the two flow rates used. An average decrease of 4% in the final concentration is observed.

The flow rate measurements provide unique insight into the complexity of the behavior of asphaltenes within the alumina porous network. Even a system as simple as the one studied shows more variance in the results than would be expected. While interpretation is not immediately evident, it is clear that the flow rate does have an observable influence on the concentration of asphaltenes in the mobile phase and, thus, on the amount adsorbed within the column. The amount of asphaltene adsorbed is around 10% higher at 0.1 ml/min than at 0.2 ml/min.

In concert, and with hopes of consolidating further evidence on the subject-matter of the present study, other the techniques than the ones previously mentioned were attempted. Obtaining substantial results from pulsed-filed gradient nuclear magnetic resonance (PFG-NMR) experiments proved to be quite difficult as no signal was recovered from the measurements of asphaltene diffusion within an alumina extrudate saturated under the same conditions as the ones used in the flow-rate measurements. Likewise, dynamic size-exclusion chromatography measurements were attempted under the same preparation methods. The strong, partially irreversible adsorption with the alumina surface, while representative of real asphaltene fractions, complicates many of the measurements as, in adsorbing conditions, dynamic method measurements are usually performed with weakly adsorbing molecules, showing clear gaussian [30] or exponentially modified gaussian peaks [31,32]. It is known that the strongest adsorption occurs as hydrogen bonding of the acidic functionalization onto the alumina surface. This means that at the moment of adsorption, the dimerization equilibrium is shifted toward dissociation as single asphaltene molecules strongly adsorb.

4. Conclusion

As expected, asphaltenes are remarkably challenging molecules to study. Working with the model molecule presents several advantages, such as a comparatively simple aggregation process and straightforward adsorption mechanism.

Most of the vital information about C5PeC11's adsorption behavior, such as isotherms, kinetics, and thermodynamic information, was obtained without any major problems. Much of the work on asphaltenes described in the literature was done using diffusion cells, with several different samples of crude from different geological origin and, consequently, without much consensus. This study intended to use a model molecule to circumvent this issue and thoroughly describe their behavior using thermodynamic and kinetic approaches. The model asphaltene behaves differently from the real fraction when it comes to surface interactions, or rather, they model only one type of molecule which is possibly present within an extracted asphaltene fraction, rather than the entire mixture.

Adsorption experiments revealed a strong affinity for alumina and relatively quick adsorption kinetics, greatly delayed by diffusional resistances. It seems that the model molecule is a good choice for kinetics point of view whereas a clear difference is obtained at the level of interaction with the surface and, consequently, at the level of thermodynamics parameters.

Finally, the influence of flow rate on adsorption has been studied, which is rarely considered, and an effect is observed that can be interpreted by friction effects on surface aggregates and/or unplugging pores in which clusters could accumulate.

Acknowledgement

The authors thank Dr. Sébastien Simon and Johan Sjöblom of the Ugelstad Laboratory, Norwegian University of Science and Technology (NTNU) who provided the model asphaltene molecule.

References

[1] J. J. Adams, Asphaltene Adsorption, a Literature Review, Energy Fuels 28 (2014) 2831–2856. https://doi.org/10.1021/ef500282p

[2] J. G. Speight, 2007. *The Chemistry and Technology of Petroleum*. 4th ed. Chemical Industries, v. 114. Boca Raton: CRC Press/Taylor & Francis.

[3] M. Marafi, H. Al-Sheeha, S. Al-Omani, A. Al-Barood, Fuel process. technol. 90 (2009). https://doi.org/10.1016/j.fuproc.2008.10.001

[4] J. Eyssautier, I. Hénaut, P. Levitz, D. Espinat, L. Barré, Energy Fuels 26 (2012) 2696–2704. https://pubs.acs.org/doi/10.1021/ef201412j

[5] K. Oh, S. C. Oblad, F. V. Hanson, M. D. Deo, Energy Fuels 17 (2003) 508–509. https://doi.org/10.1021/ef020138y

[6] O. C. Mullins, H. Sabbah, J. Eyssautier, A. E. Pomerantz, L. Barré, A. B. Andrews, Y. Ruiz-Morales, F. Mostowfi, R. McFarlane, L. Goual, R. Lepkowicz, T. Cooper, J. Orbulescu, R. M. Leblanc, J. Edwards, R. N. Zare, Energy Fuels 26 (2012) 3986–4003. https://doi.org/10.1021/ef300185p

[7] J. Castillo, M.A. Ranaudo, A. Fernández, V. Piscitelli, M. Maza, A. Navarro, Colloids and Surfaces A: Physicochemical and Engineering Aspects 427 (2013) 41-46. https://doi.org/10.1016/j.colsurfa.2013.03.016.

[8] D. Pradilla, S. Simon, J. Sjöblom, J. Samaniuk, M. Skrzypiec, J. Vermant, Langmuir 32 (2016) 2900–2911. https://doi.org/10.1021/acs.langmuir.6b00195

[9] D. Pradilla, S. Subramanian, S. Simon, J. Sjöblom, I. Beurroies, R. Denoyel, Langmuir 32 (2016), 7294–7305. https://doi.org/10.1021/acs.langmuir.6b00816

[10] S. Simon, D. Wei, M. Barriet, J. Sjoblom, Physicochem engin. aspects. 494 (2016)108-115. https://doi.org/10.1016/j.colsurfa.2016.01.018

[11] H. Toulhoat, P. Raybaud. 2013. *Catalysis by Transition Metal Sulphides - from Molecular Theory to Industrial Application*. Paris: Technip.

[12] A. Morgado Lopes, V. Wernert, L. Sorbier, V. Lecocq, M. Antoni, R. Denoyel, Mic. Mes. Mat. 310 (2021) 110640. https://doi.org/10.1016/j.micromeso.2020.110640

[13] V. G. Santos, M. Fasciotti, M. A. Pudenzi, C. F. Klitzke, H. L. Nascimento, R. C. L. Pereira, W. L. Bastosc, M. N. Eberlin, Analyst 141 (2016) 2767-2773. https://doi.org/10.1039/C5AN02333E.

[14] AFNOR NF T60-115, January 2000 - PRODUITS PETROLIERS - DOSAGE DES ASPHALTENES PRECIPITES PAR L'HEPTANE NORMAL

[15] G. Taylor, Proceedings of the Royal Society of London. Series A, Mathematical and physical sciences 225 (1954) 473-477. https://doi.org/10.1098/rspa.1954.0216

[16] R. Denoyel, F. Rouquerol, J. Rouquerol, J. colloid and interf. sci. 136 (1990) 375-384. https://doi.org/10.1016/0021-9797(90)90384-Z

[17] M. Tayakout, C. Ferreira, D. Espinat, S. Arribas Picon, L. Sorbier, D. Guillaume, I. Guibard, Chem. engin. Sci. 65 (2010) 1571-1583. https://doi.org/10.1016/j.ces.2009.10.025

[18] F. Gaulier, 2016. “Etude de la diffusion des charges lourdes en conditions réelles dans les catalyseurs d’hydrotraitment.” Université Claude Bernard Lyon 1.

[19] E. Czarnecka, J.E. Gillott, J.E. Clays Clay Miner. 28 (1980) 197–203. https://doi.org/10.1346/CCMN.1980.0280305

[20] F. Melo Faus, P. Grange, B. Delmon, Applied catalysis 11 (1984) 281 - 293. https://doi.org/10.1016/S0166-9834(00)81886-2

[21] A. Morgado Lopes, 2018, Reactive Transport Through Nanoporous Materials, Aix Marseille University

[22] K. Long Nguyen, V. Wernert, A. Morgado Lopes, L. Sorbier, R. Denoyel, Mic. Mes. Mat. 293 (2020) 109776 https://doi.org/10.1016/j.micromeso.2019.109776.

[23] S. Kokal, T. Tang, L.r Schramm, S. Sayegh, Colloids and Surfaces A: Physicochemical and Engineering Aspects 94 (1995) 253-265. https://doi.org/10.1016/0927-7757(94)03007-3
[24] D. Hallen, I. Wadsoe, D.J. Wasserman, C.H. Robert, S.J. Gill, J. Phys. Chem. 92 (1988) 3623–3625. https://doi.org/10.1021/j100323a058
[25] F. Rouquerol, J. Rouquerol, K. S. W. Sing, P. Llewellyn, G. Maurin, 2012, *Adsorption by Powders and Porous Solids*. 2nd ed. Academic Press
[26] F. Gritti, G.Guiochon, J. Chrom. A, 1069 (2005) 31-42. https://doi.org/10.1016/j.chroma.2004.08.129
[27] S. Ghorai, K. K. Pant, Sep. Pur. Technol. 42 (2005) 265-271. https://doi.org/10.1016/j.seppur.2004.09.001.
[28] E. Malkoc, Y. Nuhoglu, M. Dundar, J. hazardous mat. 138 (2006). https://doi.org/10.1016/j.jhazmat.2006.05.051
[29] N. Mohammed, N. Grishkewich, H. A. Waeijen, R. M. Berry, K. Chiu Tam, Carbohydrate Polymers 136 (2016) 1194-1202. https://doi.org/10.1016/j.carbpol.2015.09.099
[30] V. Wernert, R. Bouchet, R. Denoyel, Mic. Mes. Mat. 140 (2011) 97-102. https://doi.org/10.1016/j.micromeso.2010.09.016.
[31] J.G. Dorsey, Editorial on "Mass transfer kinetics, band broadening and column efficiency" by F. Gritti and G. Guiochon, J. Chrom. A 1221 (2012). https://doi.org/10.1016/j.chroma.2011.11.004.
[32] N. Lambert, I. Kiss, A. Felinger, J. Chrom. A 1366 (2014) 84-91. https://doi.org/10.1016/j.chroma.2014.09.025.

List of tables

Table 1 – Surface characterization of the alumina solids used (Morgado Lopes et al. 2021)

Sample	Source	v_v / mL.g^{-1}	v_{meso} / mL.g^{-1}	v_{macro} / mL.g^{-1}	d_{meso} /nm	d_{macro} /nm	S_{BET} / m².g^{-1}
Powder	Merck	0.27	0.27/ 0.25[a]	-	5.1 / 5.1[a]	-	118[a]
Extrudate	IFPEN	0.92	0.62 / 0.67[a]	0.30	8.7 / 8.5[a]	852.5	180[a]

[a] values obtained with N_2 physisorption; all other values obtained with Hg porosimetry

Table 2 – Best fit Langmuir model parameters for C5PeC11 adsorption isotherms

	Γ_{max} (mg.m^{-2})	b_0	ΔG^0 (kJ.mol^{-1})
Powder	1.16	5.12×10^5	-32.59
Extrudate (Untreated)	1.12	8.66×10^3	-22.47
Extrudate (Treated)	1.61	1.01×10^4	-22.86

Table 3 - Best fit Langmuir model parameters for RC7 adsorption isotherms

	Γ_{max} (mg.m^{-2})	b_0	ΔG^0 (kJ.mol^{-1})
Extrudate (Untreated)	0.44	505.5	-15.43
Extrudate (Treated)	0.29	528.7	-15.54

Table 4 – Best fit parameters for dissociation model

K_d (mol.L^{-1})	ΔH_d (kJ.mol^{-1})	ΔG_d (kJ.mol^{-1})	ΔS_d (J.mol^{-1}.K^{-1})
0.021	22.5	-9.5	107.4

List of figures

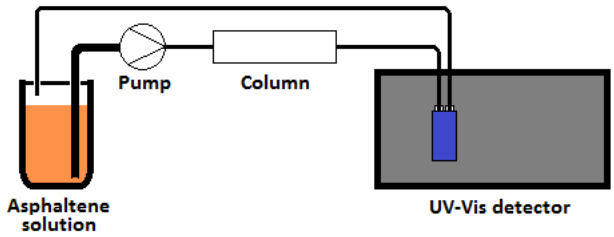

Figure 1 – Spectrophotometry setup

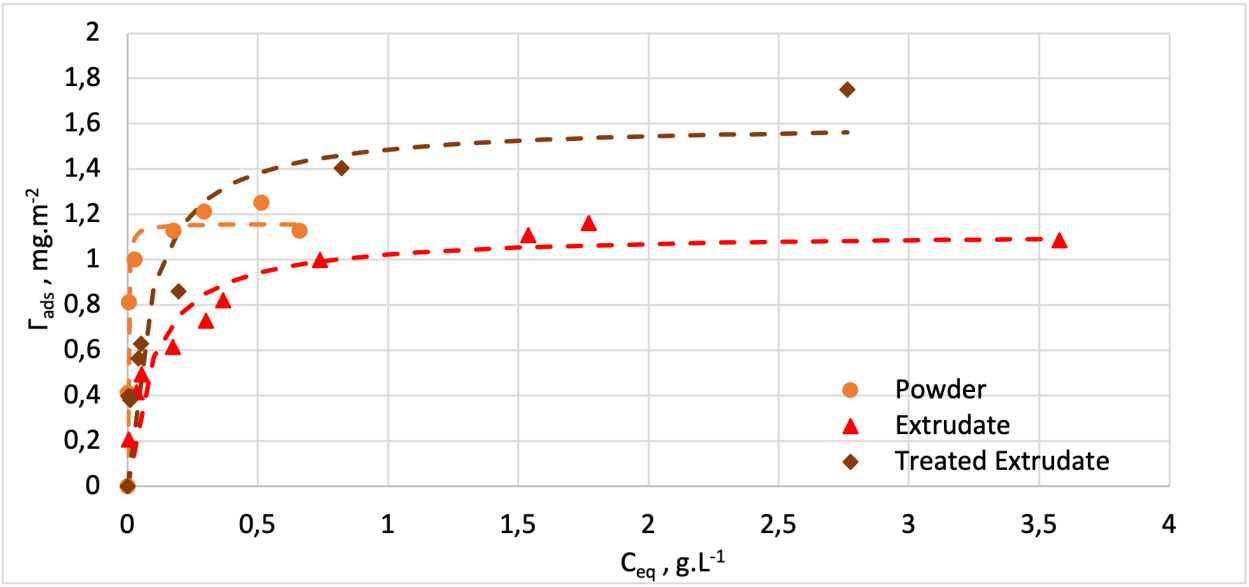

Figure 2 – Adsorption isotherms of C5PeC11 at 25°C for alumina powder, extrudate and treated extrudate (dashed lines are best approximations of the Langmuir adsorption model)

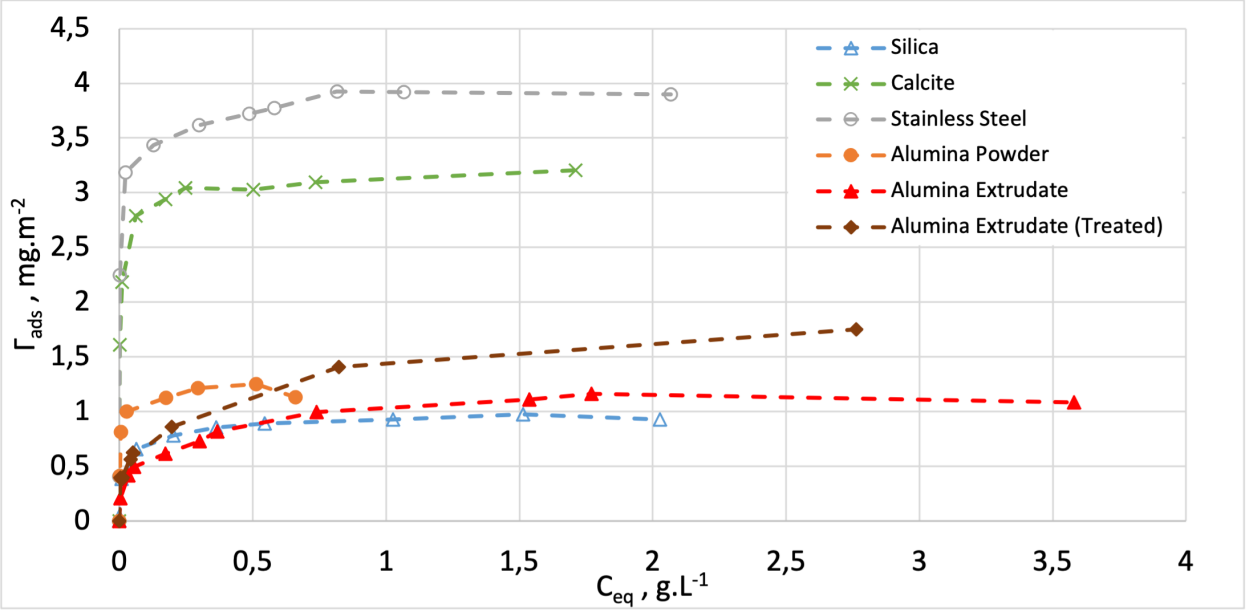

Figure 3 - Adsorption isotherms of C5PeC11 on different surfaces at 25 °C; results on silica, calcite and stainless steel are taken from Pradilla et al. 2016

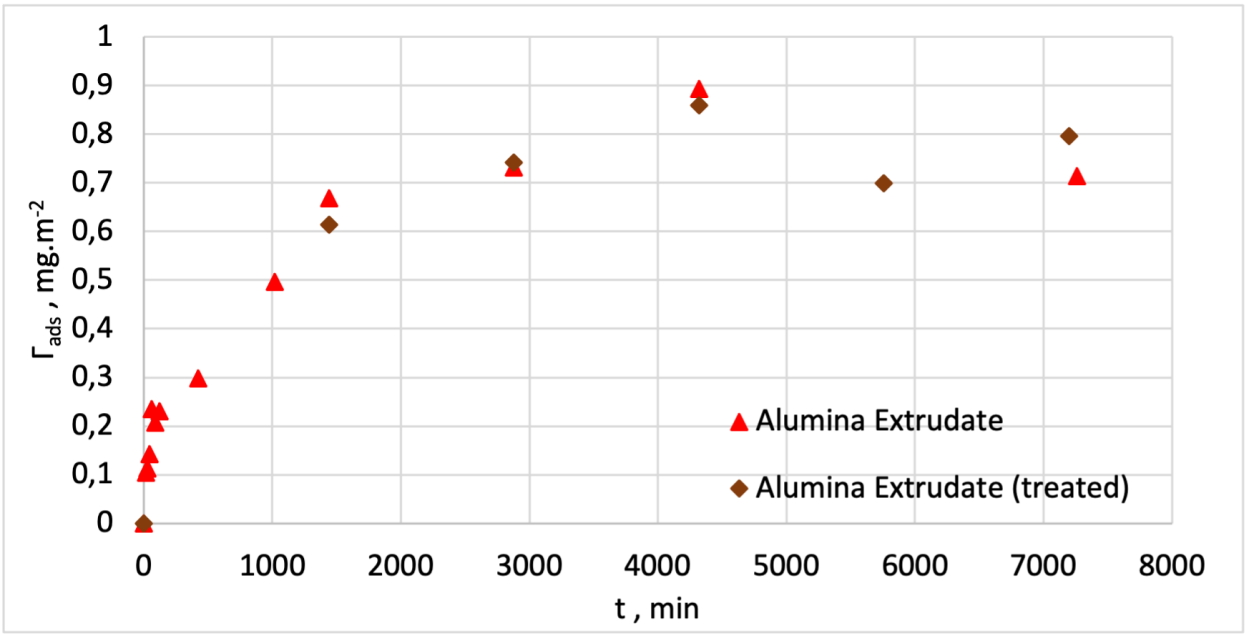

Figure 4 – Kinetics of adsorption for C5PeC11 on untreated and treated alumina extrudate

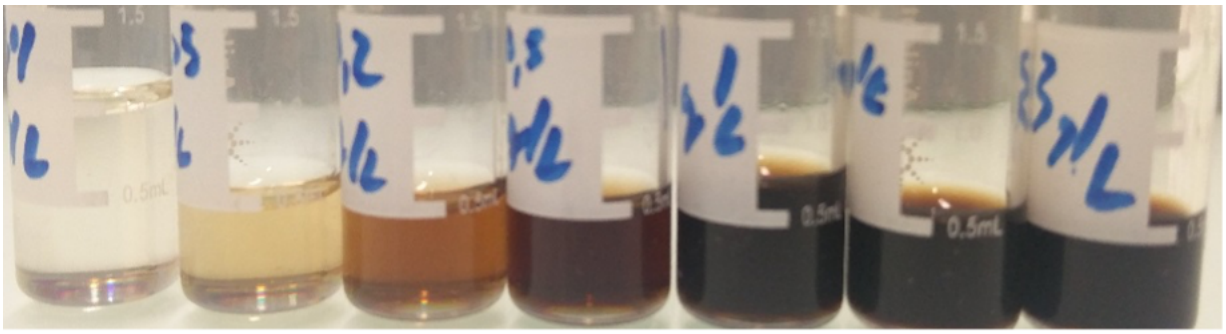

Figure 5 – Solutions of RC7 in toluene at concentrations ranging from 0.01 $g.L^{-1}$ to 3 $g.L^{-1}$

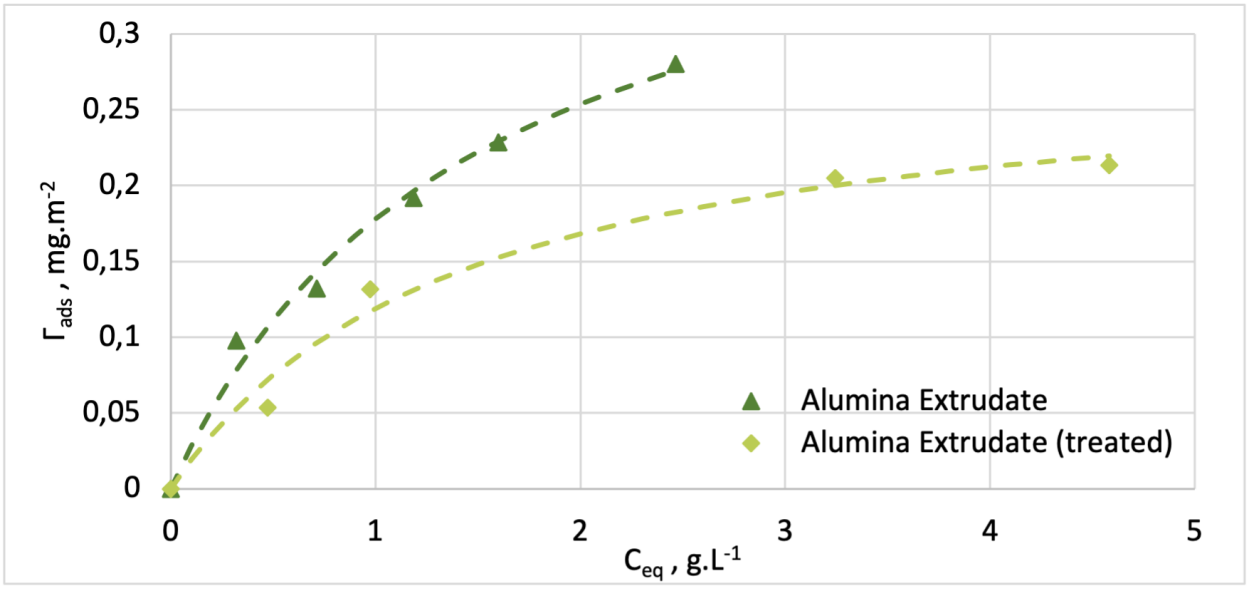

Figure 6 – Adsorption isotherms obtained with RC7 on untreated and treated alumina extrudates

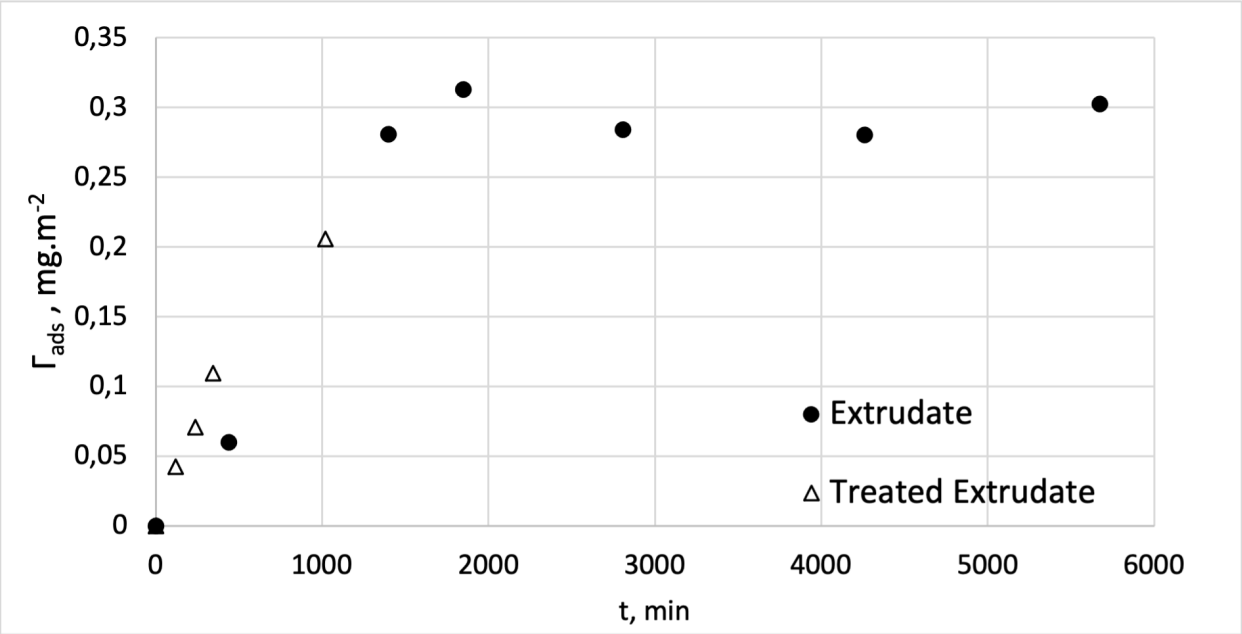

Figure 7 – Kinetics of adsorption of RC7 on untreated and treated alumina extrudates

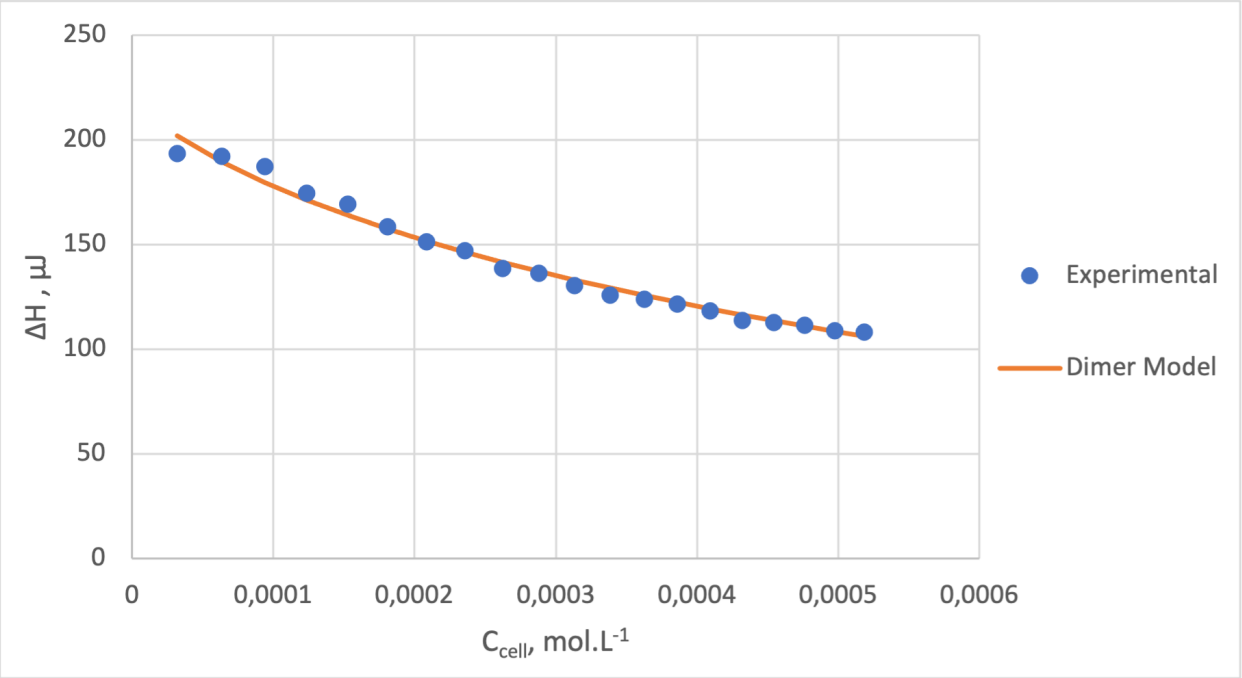

Figure 8 – Heat of dilution and dimerization model fitting

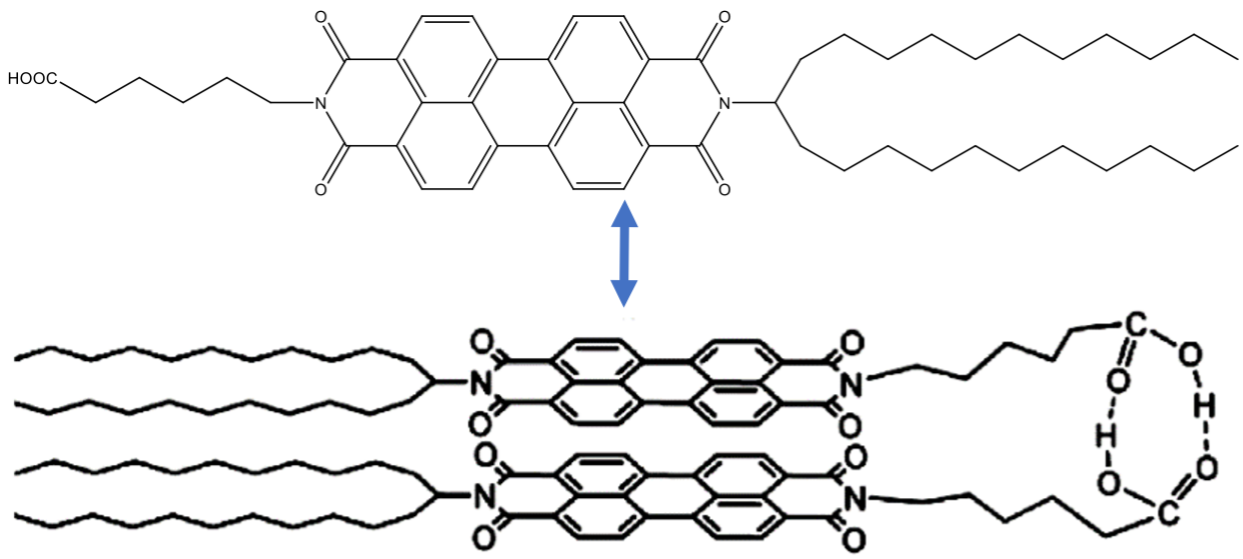

Figure 9 – Structure of the C5PeC11 dimer (Simon et al. 2016)

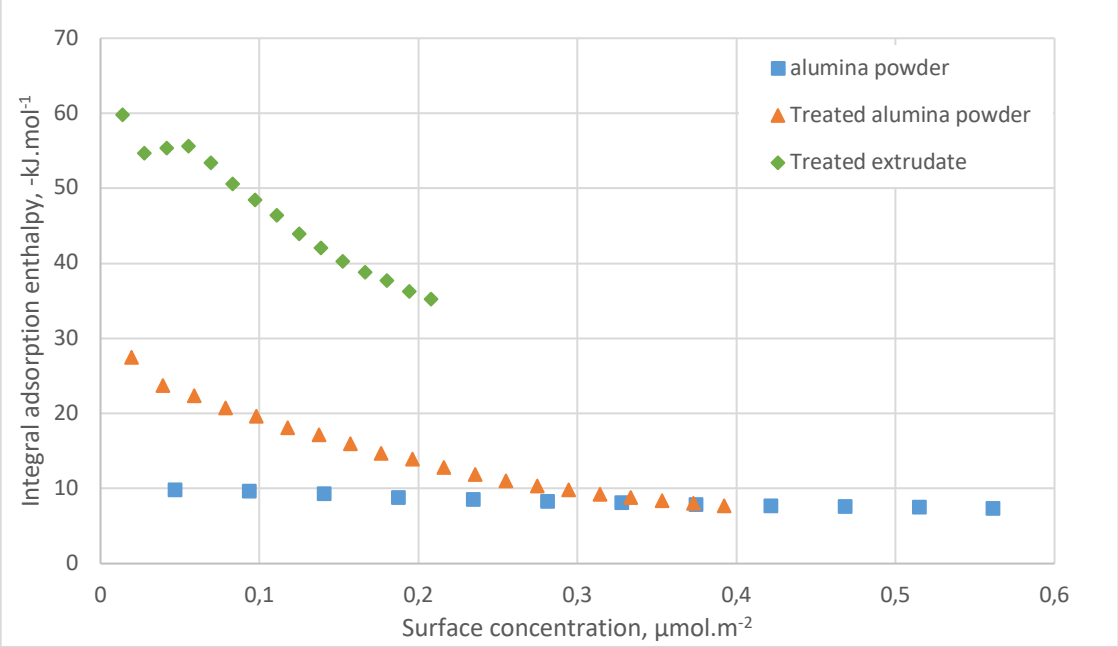

Figure 10 – Calorimetry results for the adsorption of C5PeC11 in different alumina surfaces

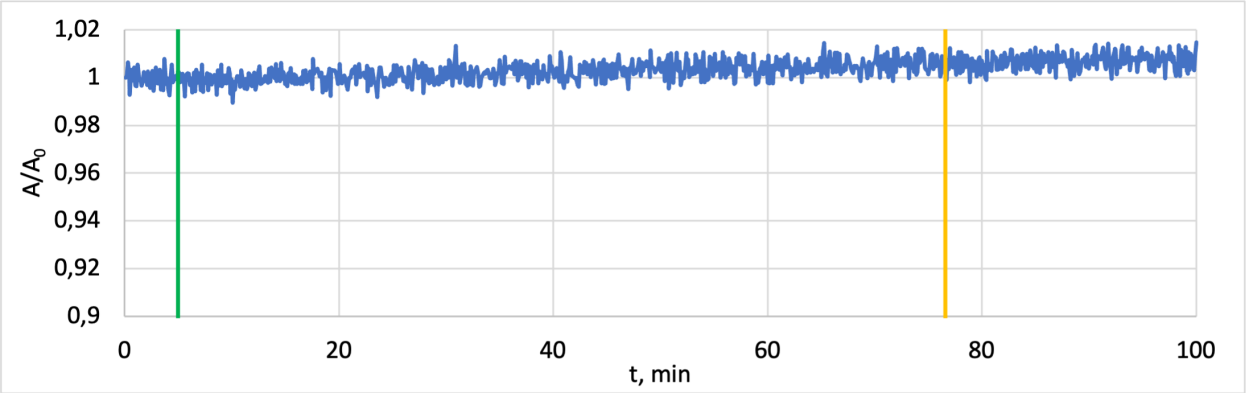

Figure 11 – Absorbance over time without column: green - flow rate change @ 5 min from 0.1 mL.min^{-1} to 0.2 mL.min^{-1}; yellow - flow rate change @ 76 min from 0.2 mL.min^{-1} back to 0.1 mL.min^{-1}.

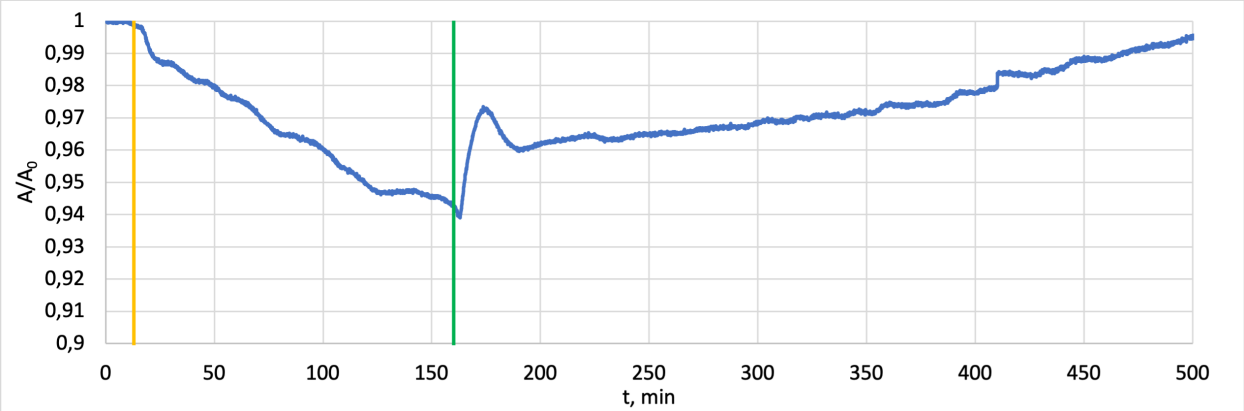

Figure 12 – Absorbance over time in 360 Mono-8: yellow – flow rate change @ 13 min from 0.2 mL.min^{-1} to 0.1 mL.min^{-1}; green - flow rate change @ 160 min from 0.1 mL.min^{-1} back to 0.2 mL.min^{-1}

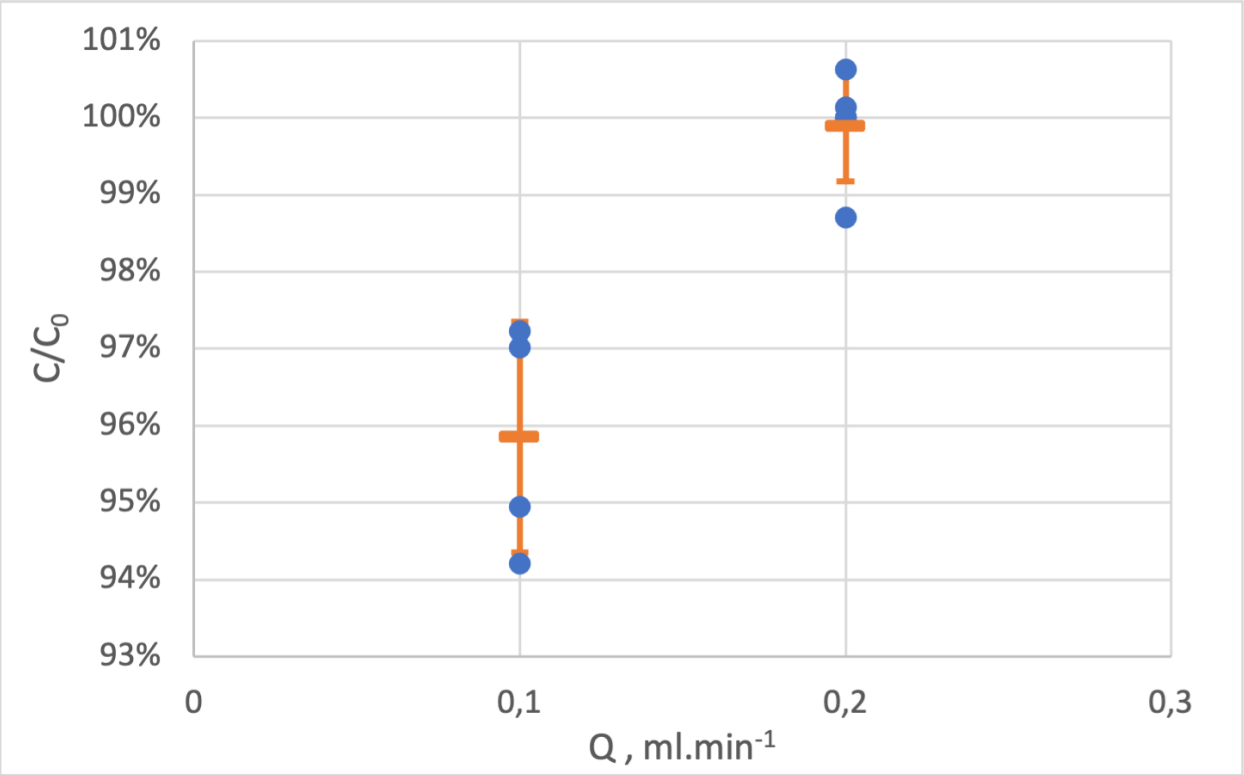

Figure 13 – Relative concentrations observed at equilibrium for the different flow rates through different experiments (blue) and average with error bars equal to the standard deviation (orange)